Shallow seismic imaging of folds above the Puente Hills blind-thrust fault, Los Angeles, California

Thomas L. Pratt
U. S. Geological Survey, School of Oceanography, University of Washington, Seattle, WA, USA

John H. Shaw
Department of Earth and Planetary Sciences, Harvard University, Cambridge, MA, USA

James F. Dolan and Shari A. Christofferson
Department of Earth Sciences, University of Southern California, Los Angeles, CA, USA

Robert A. Williams and Jack K. Odum
U. S. Geological Survey, Denver Federal Center, Denver, CO, USA

Andreas Plesch
Department of Earth and Planetary Sciences, Harvard University, Cambridge, MA, USA

Received 2 November 2001; revised 17 February 2002; accepted 17 February 2002; published 8 May 2002.

[1] High-resolution seismic reflection profiles image discrete folds in the shallow subsurface (<600 m) above two segments of the Puente Hills blind-thrust fault system, Los Angeles basin, California. The profiles demonstrate late Quaternary activity at the fault tip, precisely locate the axial surfaces of folds within the upper 100 m, and constrain the geometry and kinematics of recent folding. The Santa Fe Springs segment of the Puente Hills fault zone shows an upward-narrowing kink band with an active anticlinal axial surface, consistent with fault-bend folding above an active thrust ramp. The Coyote Hills segment shows an active synclinal axial surface that coincides with the base of a 9-m-high scarp, consistent with tip-line folding or the presence of a backthrust. The seismic profiles pinpoint targets for future geologic work to constrain slip rates and ages of past events on this important fault system. *INDEX TERMS:* 7230 Seismology: Seismicity and seismotectonics; 7223 Seismology: Seismic hazard assessment and prediction; 7221 Seismology: Paleoseismology

1. Introduction

[2] Blind-thrust faults, in which the fault does not reach the surface, pose a substantial seismic risk to the >12 million people of the Los Angeles urban area of California [*Davis et al.*, 1989; *Dolan et al.*, 1995; *Shaw and Suppe*, 1996]. This area is underlain by several blind fault systems capable of generating M_w6.5 to M_w7.6 earthquakes [*Dolan et al.*, 1995; *Shaw and Shearer*, 1999]. Most recently, a blind thrust fault ruptured in the M_w6.7 Northridge earthquake, causing over $40 billion in damages and 33 deaths [*Scientists of USGS and SCEC*, 1994; *Eguchi et al.*, 1988].

[3] The newly recognized Puente Hills thrust fault system (PHT) may be the most menacing blind fault system in the Los Angeles region because it lies directly beneath densely urbanized areas, including downtown Los Angeles (Figure 1). *Shaw and Shearer* [1999] used earthquake relocations and industry seismic reflection profiles to define the PHT, which links surface folds south and southeast of downtown Los Angeles with the deep 1987 Whittier Narrows (M_w6.0) earthquake hypocenter [*Hauksson and Jones*, 1989]. The PHT comprises the Los Angeles, Santa Fe Springs, and Coyote Hills segments (Figure 1), each of which is capable of generating M_w6.5 earthquakes individually, or a M_w7.0 earthquake if they rupture simultaneously [*Shaw and Shearer*, 1999].

[4] Industry seismic reflection data show the PHT as a series of north-dipping fault planes overlain by fault-related anticlinal folds (Figures 2a and 3a). The thrust faults dip 25° to 30° to the north and terminate upward at 3 to 4 km depth beneath the southern edge of the anticlines. The industry seismic reflection profiles and well data show that Quaternary sediments thin over the anticlines (Figures 2a and 3a), consistent with Quaternary fault motion. Above the upper terminus of the fault ramp, slip is consumed by folding within distinct kink bands that progressively narrow upwards into syntectonic (growth) strata (Figures 2a and 3a). The late Quaternary slip history of the PHT is potentially recorded in the shallow sediments at the narrow band of folding above the forelimbs, and should be discernable from detailed analyses of the fold geometry combined with age control on the shallow sediments.

[5] Unfortunately, the shallowest sedimentary strata above the tip of the PHT are not visible on the industry seismic data, which image the 300 m to 7 km depth range. The industry data therefore do not reveal whether the folds deform the shallowest strata (<300 m) or whether shallow deformation occurs at discrete axial surfaces. A south-facing slope with ~9 m of elevation change overlies the kink band along part of the Coyote Hills segment of the fault, suggesting that folding has reached the surface, but the precise relationship between this slope and any shallow deformation was unknown.

[6] In this study, we use high-resolution seismic reflection profiling to determine whether the shallowest strata above the tip of the PHT are deformed by fault-related folding, and if so, to accurately locate the axial surfaces in the shallow subsurface. Documentation of shallow folding will confirm that specific fault segments have been active in the late Quaternary. The combination of industry and shallow seismic data will also locate and define the fold geometry as it extends into the shallow subsurface, thus guiding subsequent geologic studies of the late Quaternary slip history of the PHT.

2. Data

[7] We collected high-resolution seismic reflection profiles above the Santa Fe Springs and Coyote Hills segments of the PHT (Figure 1). The Santa Fe Springs profiles (Figure 2) were acquired along Carfax Avenue in Bellflower, ~100 m west of an

0094-8276/02/2001GL014313$05.00

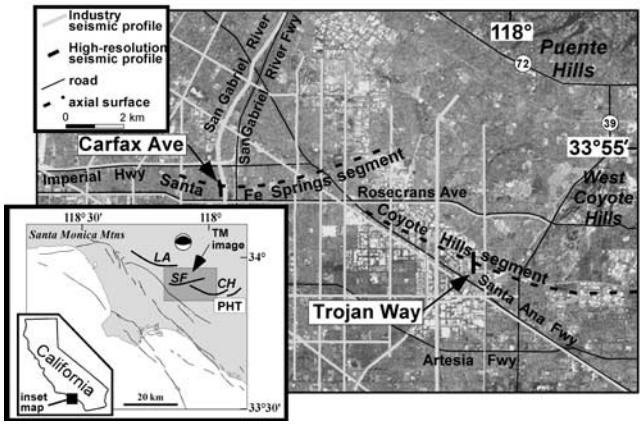

Figure 1. LandsatTM image of eastern Los Angeles, California, showing traces of the axial surfaces above the Puente Hills blind-thrust fault, locations of the industry seismic lines, and locations of the high-resolution seismic reflection profiles. Industry profiles pictured in Figures 2 and 3 are shown as bold gray lines. The inset map shows the study area relative to downtown Los Angeles (LA), and the location and focal mechanism of the 1987 Whittier Narrows earthquake (M6.0). Fault segments are labeled as LA (Los Angeles), SF (Santa Fe Springs) and CH (Coyote Hills).

industry profile [*Shaw and Shearer*, 1999]. The Carfax profiles begin ~170 m north of Rosecrans Avenue, and extend north for 672 m to a concrete wall. The Coyote Hills profiles (Figure 3) were acquired along Trojan Way where it crosses an ~9 m high, south-facing topographic slope in La Mirada. The Trojan Way profiles extend southward for 792 m from a starting point 15 m south of the intersection of Trojan Way and Alondra Boulevard. An industry profile ~1.2 km to the west of Trojan Way best shows the growth triangle in this area (Figure 3a).

[8] We used a 60-channel seismic system with a Mini-Sosie [*Barbier*, 1983; *Stephenson et al.*, 1992] or weight drop source to image the 30 to 600 m depth range, and with a hammer source to image the 10 to 100 m depth range (Figures 2 and 3; Table 1). Geophones were placed along the side of the road on which the source was used. Distance annotations (Figures 2b, 2c and 3b) refer to the starting points of the Mini-Sosie profiles.

[9] On Carfax Avenue we used three earth tampers as a Mini-Sosie system. We recorded 72 sec of data (~1200 impacts) and cross-correlated the data with a record of the impacts to synthesize an impulsive source. For the hammer profile, we used a 4.5 kg (10 lb) sledgehammer and summed two impacts at each source-point along the flat, straight road. The hammer profile started 60 m from the south end of the Mini-Sosie profile.

[10] For the northern part of the Trojan Way profile, we used four impacts of a 100-kg, vacuum-assisted weight drop at each sourcepoint. The weight drop had mechanical failure at station 198 (distance 388 m), and we completed the profile using the Mini-Sosie system with the same acquisition parameters as the Carfax profile. For the hammer profile, we summed 8 impacts per sourcepoint to suppress the substantial traffic and electrical noise that was present, but the data were still plagued by noise. Source and receiver points were surveyed.

[11] Data processing was routine for seismic reflection profiles (Table 1; *Yilmaz* [1987]), and included residual statics corrections, pre- and post-stack deconvolution, eigenvector filter, Stolt time migration, and time-to-depth conversion. Stacking adjacent traces further increased the signal-to-noise ratio.

[12] On the shot records, shallow events showed hyperbolic moveout characteristic of reflections. The dipping events on the north side of the Trojan Way Mini-Sosie section (Figure 3b) are obscured on individual shot records by traffic and electrical noise, but they appear to be reflections because they have reasonable stacking velocities, lie below a clear reflection, and are not removed by deconvolution (as reverberations would be).

3. Interpretation

[13] The high-resolution seismic reflection profiles show that the growth triangles (kink bands) above the tip of the PHT extend into the shallow strata (<300 m) near the locations predicted from interpretation of the industry seismic lines (Figures 2 and 3). The growth triangles include discrete zones of dipping strata with well-

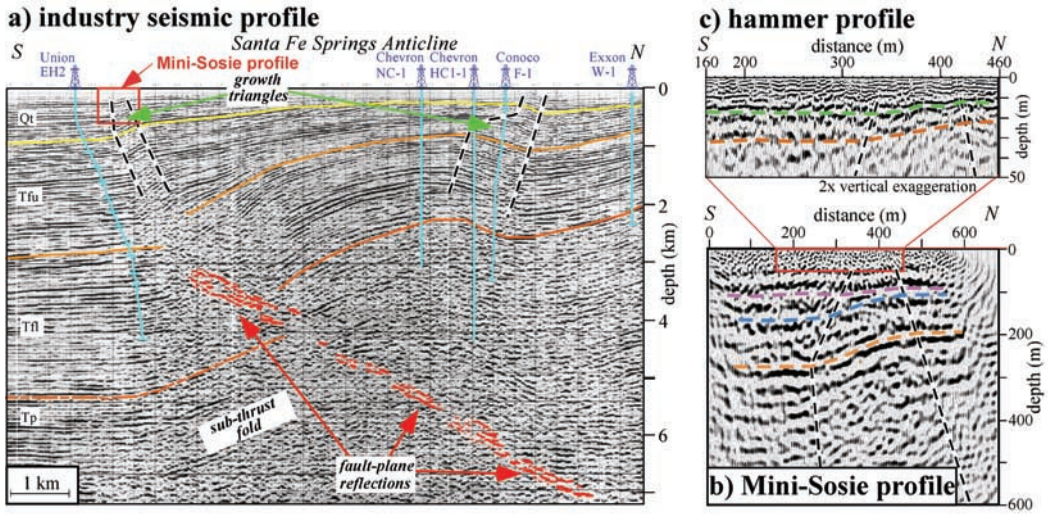

Figure 2. Carfax Avenue seismic reflection profiles (migrated). The profiles show discrete anticlinal and synclinal axial surfaces (dashed lines) that define an upward-narrowing kink band at the forelimb of the Santa Fe Springs anticline above the Puente Hills fault zone. Colored lines on the industry profile show stratigraphic boundaries; colored lines on the high-resolution profiles denote prominent reflections. The hammer profile has a 2× vertical exaggeration, other profiles have no vertical exaggeration. The top of the industry profile is at sea level; the tops of the high-resolution profiles are at an elevation of 27 m (the ground surface). Horizontal scale is the distance from the south end of the Mini-Sosie profile. Qt = Quaternary; Tfu = Pliocene upper Fernando Formation; Tfl = Pliocene lower Fernando Formation; Tp = Miocene Puente Formation. Industry data courtesy of Texaco, Inc.

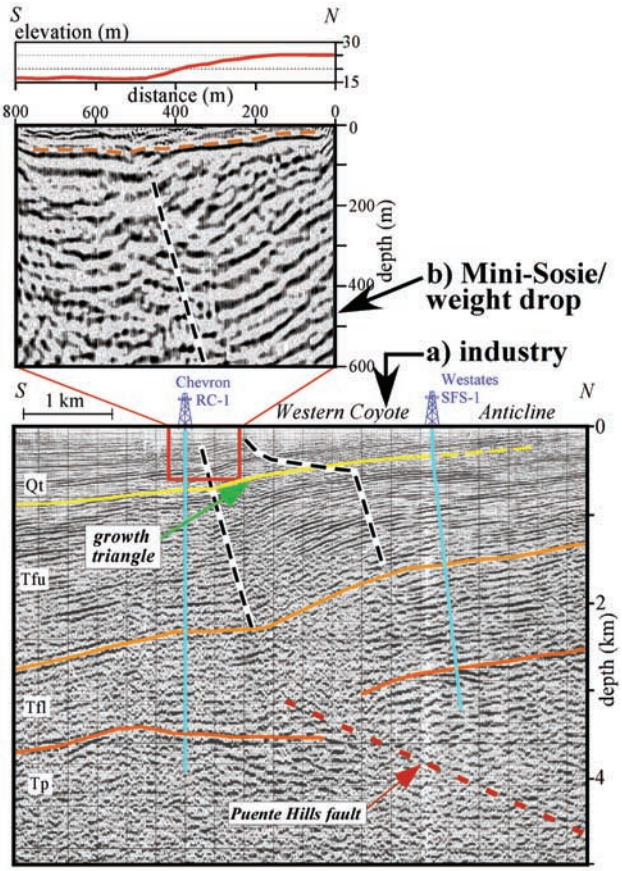

Figure 3. Seismic reflection profiles across the Coyote Hills segment of the Puente Hills thrust fault (migrated and plotted with no vertical exaggeration). Colored lines on the industry profile show stratigraphic boundaries; the colored line on the high-resolution profile denotes a prominent reflection interpreted to be from an unconformity. The profiles show an upward-narrowing kink band whose synclinal axial surface corresponds with the base of a south-facing scarp. Qt = Quaternary; Tfu = Pliocene upper Fernando Formation; Tfl = Pliocene lower Fernando Formation; Tp = Miocene Puente Formation. Industry data courtesy of Texaco, Inc.

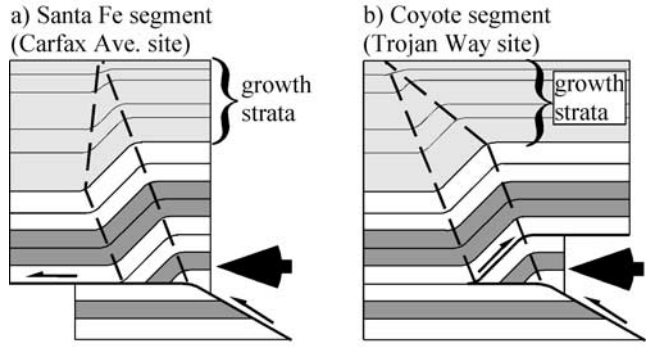

Figure 4. Balanced models showing our interpretations of the kink band geometry above the Santa Fe Springs (left) and Coyote Hills (right) segments the Puente Hills thrust fault. The kink band imaged at the Carfax Avenue site is a forelimb fault-bend fold with an active anticlinal axial surface above the fault bend. The growth triangle at the Trojan Way site (right) forms from tip-line folding, with an active synclinal axial surface above a wedge zone where slip is transferred from the deep ramp to a backthrust. Large arrows show the direction of motion of the hanging wall of the main thrust fault; small arrows show the sense of motion on individual faults.

defined axial surfaces, indicating that fold growth has occurred during deposition of these upper Quaternary strata. Coincidence of the active synclinal axial surface and the base of the topographic slope at the Trojan Way profile is consistent with uplift and folding of the surface during fault motion. Acquisition of more precise age control on the upper Quaternary sediments is the goal of an ongoing companion study [*Christofferson et al.*, 2000, 2001].

[14] The Carfax Avenue profiles (Figure 2) show the growth triangle narrowing as it extends upward into progressively younger deposits. The Mini-Sosie profile shows a well-defined kink band in the prominent reflector at 200 to 280 m depth (orange dashed line, Figure 2b). The kink band at this prominent reflector is ~270 m wide, and exhibits a total of ~80 m vertical uplift across the deformed zone. The strata dip ~17° to the south within the kink band. The growth triangle may also be expressed at ~90 m depth on the Mini-Sosie profile, where a prominent reflector dips gently to the south between distance marks 320 and 460 m (purple dashed line, Figure 2b). An unconformity is interpreted at ~100 m depth, where large differences in reflector dip suggest sediments are missing (between the purple and blue dashed lines in Figure 2b).

[15] On the Carfax hammer profile (Figure 2c), reflectors appear to dip gently to the south above the updip projection of the growth triangle. For reflectors at 10 to 20 m depth, this dip panel appears to be localized between distance marks 330 and 420 m. These relationships suggest that the active axial surface extends to within 20 m of the surface as a discrete zone. Shot records also suggest a southward dip to the reflectors that does not appear to be caused by lateral velocity changes. We are collecting borehole data to determine the lithologies of these reflectors and estimate the depth to the water table [*Christofferson et al.*, 2000, 2001].

[16] The Trojan Way profiles (Figure 3) show the active, synclinal axis of the growth triangle extending upwards from the fold imaged by the industry data. Strata beneath the northern half of the Mini-Sosie profile dip to the south at apparent angles of up to 30° (Figure 3b), but stacking velocities, and thus the dip angle, are not well determined on these relatively noisy data. Strata in the growth triangle imaged on the industry data dip ~20° south. Reflectors beneath the southern half of the Mini-Sosie profile are nearly flat. The position of the synclinal axial surface is defined by the ~100-m-wide transition between the dipping and flat reflectors on the deeper portions of the seismic section. The kink band is at least 300 m wide

Table 1. Key Acquisition and Processing Parameters

Line Name	Line length (m)	Station Spacing (m)	Sample rate (msec)	Trace length (sec)	Bandpass Filter (Hz)	Decon (gap, filter length) (msec)
Carfax Mini-Sosie	672	4	1.0	1.0	12-24-80-160	16, 100
Carfax hammer	450	1	0.5	0.5	40-80-240-480	8, 100
Trojan Way Mini-Sosie	792	4	1.0	1.0	10-20-60-120	18, 300
Trojan Way hammer	300	1	0.5	0.5	30-60-120-240	20, 80

in the middle and lower portions of the seismic data. We cannot determine the width of the kink band in the shallow strata. The kink band presumably continues to narrow upwards (Figure 4b), but the anticlinal axis either lies north of the Mini-Sosie/weight drop profile or the anticlinal axial surface is not a sharp fold.

[17] On the Trojan Way profiles, a strong reflector between 30 and 80 m depth appears to be an unconformity because it dips to the south at an angle of ~7° north of distance mark 450, in contrast to the ~30° dip of the underlying reflectors (Figure 3b). Near distance mark 450, this shallow reflector appears to flatten, defining the position of the active synclinal axial surface. Strata imaged near the top of the industry seismic lines clearly show a fold rather than a fault beneath this synclinal axial surface (Figure 3a). The Trojan Way hammer profile (not shown) shows the same prominent reflector as the Mini-Sosie profile at 30 to 80 m depth, but does not clearly image reflectors at shallower depths.

[18] The active, synclinal axial surface beneath Trojan Way, defined by the change in reflector dip, coincides with the base of the topographic slope (Figure 3b). This correlation suggests that the slope is related to folding that uplifted and tilted the ground north of the active axial surface.

4. Discussion

[19] The high-resolution seismic profiles demonstrate that folding above the PHT extends into the shallow sediments (<300 m) as a discrete kink band, consistent with the late Quaternary activity on the PHT implied by its projection to the hypocenter of the Whittier Narrows earthquake [*Shaw and Shearer*, 1999]. The shallow fold scarps were not associated with observable surface deformation during the 1987 Whittier Narrows (M6.0) earthquake. Thus, their presence suggests that other earthquakes that involved discrete near-surface folding have occurred on the PHT in the past. As discussed by *Shaw and Shearer* [1999], these events may have occurred as individual ruptures of single fault segments (~M_w6.5) or as multi-segment ruptures (~M_w7.0).

[20] The high-resolution seismic data also demonstrate that fold panels visible on the industry seismic data narrow upwards. This implies that the folds develop through kink-band migration [*Suppe et al.*, 1992] rather than pure limb rotation. Viable mechanisms include fault-bend folding [*Suppe*, 1983], structural wedging [*Medwedeff*, 1989], fault-propagation folding [*Suppe and Medwedeff*, 1990], and certain types of trishear folding [*Erslev*, 1991; *Allmendinger*, 1998; *Allmendinger and Shaw*, 2000].

[21] In the Carfax profiles over the Santa Fe Springs segment of the fault, the active anticlinal axial surface appears to be planar to within 70 m of the surface on the Mini-Sosie profile, and perhaps as shallow as 12 m depth on the hammer profile, consistent with an active axis in a forelimb fault-bend fold (Figure 4a). The inactive, synclinal axis converges toward the anticlinal axis because decreasing amounts of slip have occurred since the progressively younger sediments were deposited [*Suppe et al.*, 1992]. The relatively gentle dip of the shallow reflectors on the hammer line could be due to a curved-hinge geometry for the fault-bend fold [e.g., *Suppe et al.*, 1997; *Novoa et al.*, 2000]. The Trojan Way profiles across the Coyote Hills segment, in contrast, show a planar, active synclinal axial surface that is consistent with tip-line folding or structural wedging at the front of the Puente Hills thrust fault (Figure 4b; [*Erslev*, 1991; *Allmendinger*, 1998; *Allmendinger and Shaw*, 2000; *Medwedeff*, 1989]).

[22] The high-resolution seismic data serve to constrain fold kinematics, as well as locate discrete, near-surface zones of deformation that record late Quaternary deformation above the PHT. Long-term slip rates on the PHT are estimated to be 0.5 to 2.0 mm/year [*Shaw and Shearer*, 1999]. Determination of shorter-term slip rates awaits direct sampling and age dating of sediments from these shallow zones of active folding [*Christofferson et al.*, 2000, 2001].

[23] **Acknowledgments.** Phillip Armstrong of Calif. State Univ., Fullerton, lent us the weight drop. The study was funded by the U. S. Geological Survey National Earthquake Hazard Reduction Program, the University of Southern California, and Harvard University. We thank the acquisition crew of Patricia Fiore, Erik Frost, Ross Hartleb, Lisa Nousek, and Allan Tucker. Reviews by William Stephenson, Rufus Catchings, Thomas Brocher and two anonymous reviewers improved the manuscript.

References

Allmendinger, R. W., Inverse and forward numerical modeling of trishear fault-propagation folds, *Tectonics*, *17*, 640–656, 1998.

Allmendinger, R. W., and J. H. Shaw, Estimation of fault propagation distance from fold shape: Implications for earthquake hazard assessment, *Geology*, *28*, 1099–1102, 2000.

Barbier, M. G., *The Mini-Sosie Method*, International Human Resources Development Corporation, Boston, MA, 186 pp., 1983.

Christofferson, S. A., J. F. Dolan, J. H. Shaw, and T. L. Pratt, Determination of a latest Pleistocene-Holocene slip rate for the Puente Hills blind thrust fault, Los Angeles basin, California, *Eos Trans AGU*, *82*, F933, 2001.

Christofferson, S. A., J. F. Dolan, J. H. Shaw, T. L. Pratt, R. A. Williams, and J. K. Odum, Paleoseismologic investigation of a blind thrust fault, Puente Hills thrust fault, Los Angeles Basin, California: Towards a determination of Holocene slip rates and ages of individual paleoearthquakes: *Eos Trans AGU*, *81*, F850, 2000.

Davis, T. L., J. Namson, and R. F. Yerkes, A cross section of the Los Angeles area: Seismically active fold-and-thrust belt, the 1987 Whittier Narrows earthquake and earthquake hazard, *J. Geophys. Res.*, *94*, 9644–9664, 1989.

Dolan, J. F., K. Sieh, T. K. Rockwell, R. S. Yeats, J. Shaw, J. Suppe, G. J. Huftile, and E. M. Gath, Prospects for larger or more frequent earthquakes in the Los Angeles metropolitan region, *Science*, *267*, 199–205, 1995.

Eguchi, R. T., J. D. Goltz, C. E. Taylor, S. E. Chang, P. J. Flores, L. A. Johnson, H. A. Seligson, and N. C. Blais, Direct economic losses in the Northridge Earthquake: A three-year post-event perspective, *Earthquake Spectra*, *14*, 245–264, 1988.

Erslev, E. A., Trishear fault-propagation folding, *Geology*, *19*, 617–620, 1991.

Hauksson, E., and L. M. Jones, The 1987 Whittier Narrows earthquake sequence in Los Angeles, southern California, *J. Geophys. Res.*, *94*, 9569–9589, 1989.

Medwedeff, D. W., Growth fault-bend folding at southeast Lost Hills, San Joaquin Valley, California, *Am. Assoc. Petr. Geol. Bull.*, *73*, 54–67, 1989.

Novoa, E., J. Suppe, and J. H. Shaw, Inclined-shear restoration of growth folds, *Am. Assoc. Petr. Geol. Bull.*, *84*, 787–804, 2000.

Scientists of USGS and SCEC, The magnitude 6.7 Northridge, California, Earthquake of 17 January 1994, *Science*, *266*, 389–397, 1994.

Shaw, J. H., and P. Shearer, An elusive blind-thrust fault beneath metropolitan Los Angeles, *Science*, *283*, 1516–1518, 1999.

Shaw, J. H., and J. Suppe, Earthquake hazards of active blind-thrust faults under the central Los Angeles basin, California, *J. Geophys. Res.*, *101*, 8623–8642, 1996.

Stephenson, W. J., J. Odum, K. M. Shedlock, T. L. Pratt, and R. A. Williams, Mini-Sosie high-resolution seismic method aids hazards studies, *Eos Trans AGU*, *73*, 473–476, 1992.

Suppe, J., Geometry and kinematics of fault-bend folding, *Am. Jour. Science*, *283*, 684–721, 1983.

Suppe, J., and D. Medwedeff, Geometry and kinematics of fault-propagation folding, *Eclogae Geologicae Helvetiae*, *83*, 409–454, 1990.

Suppe, J., G. T. Chou and S. C. Hook, Rates of folding and faulting determined from growth strata, in *Thrust Tectonics*, edited by K. R. McKlay, pp. 105–121, Chapman Hall, New York, 1992.

Suppe, J., F. Sabat, J. A. Muñoz, J. Poblet, E. Roca, and J. Vergés, Bed-by-bed growth by kink-band migration: Sant Llorende Morunys, eastern Pyrenees, *Jour. Structural Geol.*, *19*, 443–461, 1997.

Yilmaz, O., *Seismic Data Processing*, Soc. Exploration Geophys., Tulsa, Oklahoma, 526 pp., 1987

T. L. Pratt, U. S. Geological Survey, School of Oceanography, University of Washington, Seattle, WA 98115, USA.

J. H. Shaw, Department of Earth and Planetary Sciences, Harvard University, Cambridge, MA 02138, USA.

J. F. Dolan and S. A. Christofferson, Department of Earth Sciences, University of Southern California, Los Angeles, CA 90089, USA.

R. A. Williams and J. K. Odum, U. S. Geological Survey, MS 966, Denver Federal Center, Denver, CO 80225, USA.

A. Plesch, Department of Earth and Planetary Sciences, Harvard University, Cambridge, MA 02138, USA.